C_{60} Buckminsterfullerene High Yields Unraveled

R. F. Curl,* Mi Kyung Lee, and G. E. Scuseria

Chemistry Department and Rice Quantum Institute, Rice University, Houston, Texas

Received: August 4, 2008; Revised Manuscript Received: September 19, 2008

Recently Irle, Morokuma, and collaborators have carried out a series of quantum chemical molecular dynamics simulations of carbon clustering. The results of these computer experiments are that carbon clusters of size greater than 60 atoms are rapidly formed, anneal to giant fullerenes, and then these fullerenes shrink. The simulation could not be carried to long enough times for the shrinking to reach C_{60}, but they propose reasonably that this shrinking process ultimately forms buckminsterfullerene. However, these simulations do not reveal the force driving the shrinking process. Here, this driving force for shrinking is found to be reactions in which C_2 is swapped between fullerenes. The key element is that for typical fullerenes the equilibrium constants for such C_2 interchanges are near unity, resulting in expansion of the breadth of the fullerene distribution in an annealing process. When fullerenes of 60 or 70 atoms are populated by shrinking, they fall into the local energy minimum of buckminsterfullerene or D_{5h} C_{70}. This simple mechanism accounts for the high yields (>20%) of buckminsterfullerene that can be achieved in pure carbon systems.

Introduction

In general, it is not hard to understand the formation of fullerenes. For isolated even carbon clusters containing more than about 36 atoms, the energetically most stable form will be a fullerene. Thus, a cluster in this size range with another type of structure can be expected to anneal at a high temperature to a fullerene. This phenomenon has been proposed by Bowers[1,2] as "growth and collapse."

It is far more difficult to understand the high yield of well more than 20% of the carbon vaporized that has been observed for buckminsterfullerene (henceforth $^{Ih}C_{60}$) in pure carbon systems.[3] Until recently, only the "pentagon road" mechanism proposed by Smalley[4] seems to have tackled this issue head on. Smalley imagined a valley leading directly to $^{Ih}C_{60}$. He hypothesized this energy valley is created by healing dangling bonds through pentagon formation. The fact that under some conditions $^{Ih}C_{60}$ yields are small in pure carbon systems is easily accounted for in the pentagon road mechanism by noting that the rearrangements required for pentagon formation require activation energies. Supporting this view is the fact[3,4] that high temperatures during the synthesis process are needed to obtain high yields of $^{Ih}C_{60}$.

Irle, Morokuma, and collaborators have recently proposed a different scheme for fullerene production in a series of papers[5−8] describing quantum chemical molecular dynamics simulations of carbon clustering. In these simulations, relatively large carbon clusters that resemble imperfect (often only partially closed, often with carbon chain tails) fullerenes form very rapidly, consuming most of the small carbon clusters such as C_2. In the simulations during continued high temperature exposure, the imperfections are annealed away, giving rise to perfect fullerenes, some of which begin to shrink toward $^{Ih}C_{60}$. Irle, Morokuma, and collaborators argue that these simulations provide a better explanation for $^{Ih}C_{60}$ production, which they call "size up/size down." Irle and Morokuma call the "size down" mechanism revealed by their simulations "the shrinking hot giant."

In these simulation reports, the authors seem unclear of what is driving the shrinking process[7] (see the last two pages) and perhaps somewhat unsure about what is causing the continued presence of large fullerenes[8] (see the penultimate paragraph). The purpose of this report is to propose a mechanism for this annealing process that explains both the driving force for the fullerene shrinking and how it is that large fullerenes persist. Most importantly, it provides fundamental insights into how $^{Ih}C_{60}$ can be produced in high yield in pure carbon systems. The operation of the mechanism is demonstrated by model thermodynamic and kinetic calculations.

Experimental Evidence

Before launching into a description of our model, it seems necessary to review some of the experimental evidence. Processes in which C_2 is ejected from fullerenes followed by annealing of the resulting smaller fullerene have experimental support. In a study[9] of the photophysics of fullerenes, the ability of a such a shrinking system to find the special stability of C_{60}^+ in photofragmentation was clearly demonstrated (Figure 12 of that paper). Recently, a movie has been made[10] of a fullerene shrinking.

The pentagon road hypothesis seems to be strongly contradicted, and fullerene production by some annealing process from larger fragments strongly supported by the startling observations on fullerene formation by Xie et al.,[11] who examined the residual ions produced by unfocused laser vaporization of highly ordered pyrolytic graphite into a vacuum. This study found large differences in the cluster distributions, depending on whether the ablation was from a surface with the graphene sheets perpendicular to the surface (no fullerene ion production) or parallel to it (copious C_{60} and C_{70} ion production). For the laser striking a pristine surface having the graphene sheets in its plane, C_{60} ions were produced almost exclusively. As the surface roughened by ablation, the distribution shifted to substantial production of larger even-numbered clusters and some growth of the C_{70} peak, until after 3000 shots it strongly resembled the distribution characteristic of fullerene arc synthesis soot. Because this all takes place in a good vacuum, there appears to be no

* Corresponding author. E-mail: rfcurl@rice.edu.

10.1021/jp806951v CCC: $40.75
Published on Web 10/29/2008

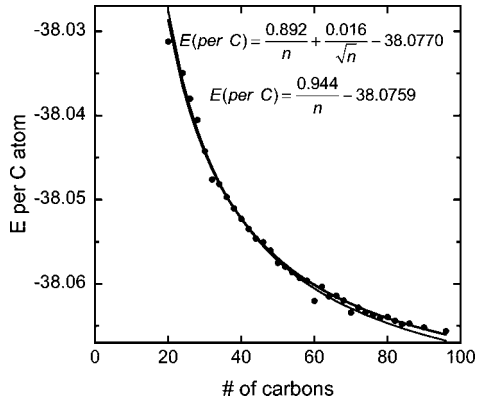

Figure 1. Energies (Hartrees) per carbon atom of the most stable fullerene isomers for a given number of atoms. The equations in the figure are fitted to the points omitting C_{60} and C_{70} and both describe the heavy line through the points. The thin line in the figure describes the result of the one parameter fitting using $E = a/n - 38.0770$ hartree.

way that the pentagon road with its requirement of building up the structure of C_{60} by a series of reactions can explain these observations. A much more plausible explanation is that initially relatively large graphene sheets are ejected from the surface with so much excess energy that they can not only rearrange to form fullerenes but are left with sufficient energy to eject small carbon species probably C_2 with surface rearrangements until they fall into the $^{Ih}C_{60}$ well (Figure 1). Perhaps the surface roughening after many shots allows multiple layer fragments to be peeled off changing the nature of the starting material.

Combustion Production of Fullerenes. $^{Ih}C_{60}$ and $^{D5h}C_{70}$ are produced commercially in large quantities using a combustion process. Lower overall yields in terms of the carbon in the fuel are to be expected in flames because much of the carbon is also being used to heat the system. Nevertheless, flame yields are high enough to make combustion systems the preferred industrial process for producing fullerenes.

The sooting flames used in combustion systems producing fullerenes do not achieve temperatures much above 2000 K. We believe that much higher temperatures are required to stay on the pentagon road. In addition in a combustion system, there are many other species such as H, OH, or carbon-containing radicals that might attach to dangling bonds removing the driving force for pentagon formation. Thus, a fullerene formation mechanism different from the pentagon road appears to be needed to account for fullerene formation in flames. But as yet we do not see how the model we propose here could be modified to apply in the more complex chemistry of flames.

Energetics of Fullerenes. In 1994, one of us (GES) carried out[12] ab initio calculations of the energies of the most stable isomers of a number of fullerenes. Because there have been significant advances in computers and quantum chemical methods in the intervening 14 years, these calculations are redone here with better methods (PBE1PBE/6−31G**). The resulting energies are plotted in Figure 1 and tabulated in the Supporting Information. In Figure 1, the energies per carbon atom with the exceptions of $^{Ih}C_{60}$ and $^{D5h}C_{70}$ have been least-squares fitted by eq 1. This is the heavy line in Figure 1.

$$E = E_1/n + E_0 \quad (1)$$

Whereas the fit is good, the form of the equation is wrong as became apparent after we calculated the energy per carbon atom (−38.07704961 hartree/atom) of an infinite graphene sheet using the PBE1PBE/6−31G**//LSDA/3−21G method and attempted to convert the two parameter fit of eq 1 to a one parameter fit by fixing E_0 to this calculated graphene value. This is the thin line in Figure 1. A more appropriate formula for fitting the energy curve is

$$E = \frac{E_v}{n} + \frac{E_e}{\sqrt{n}} + E_f \quad (2)$$

In eq 2, E_v is associated with the energies of the carbon atoms at the pentagons, which become at large n the 12 vertices of a large (usually unsymmetrical) icosahedron, E_e is associated with carbon atoms at the edges of this icosahedron, and E_f is associated with the carbon atoms on the faces of this large icosahedron (Supporting Information). This is also the thick line in Figure 1. Over the size range displayed in Figure 1, the two parameter fit by eq 1, or the two parameter fit by eq 2 (fixing E_f to the graphene value) never differ by as much as 2×10^{-4} H or 0.5 kJ/mol. At larger n, the two fits gradually diverge with the curve of eq 2 falling below that of eq 1. The parameters (in hartrees) obtained using eq 2 are $E_v = 0.892$, $E_e = 0.0161$, and $E_f = -38.07704961$ (again E_f is the energy per atom of the graphene sheet).

Obviously the energies per carbon atom of $^{Ih}C_{60}$ and $^{D5h}C_{70}$ fall below the curve that has been least-squares fitted to the energies of the other fullerenes. However, because of the overall downward trend, the energy per carbon atom of the most stable isomer (D_{6d}) of C_{72}, which falls on the curve, is below that of $^{Ih}C_{60}$.

Consider the reaction

$$nC_m \rightleftharpoons mC_n (n > m)) \quad (3)$$

According to the simple formula (1)

$$\Delta E_3 = mE_n - ne_m = mne_n - nme_m = nm(e_n - e_m) < 0 \quad (4)$$

where e_i is the energy per carbon atom. (If eq 2 is used, ΔE_3 is more negative at large n.) Thus, larger fullerenes tend to be energetically more stable than smaller ones. In particular, $^{Ih}C_{60}$ is higher in energy than at least one isomer of all fullerenes larger than C_{68}. For m corresponding to $^{Ih}C_{60}$ and n to $^{D5h}C_{70}$, we have carried out calculations that demonstrate that the inclusion of entropic effects for practical values ($>10^6$ cm^{-3}) for the sum of the concentrations of C_{60} and C_{70} does not affect the equilibrium enough to favor the smaller fullerene at 4000 K. In summary, at practical concentrations thermodynamic equilibrium among fullerenes favors giant fullerenes. Thus, it would appear to get a good yield of $^{Ih}C_{60}$ it must be directly in the growth path (the pentagon road) because thermodynamics implies there is no return from larger fullerenes. No wonder Irle, Morokuma, and co-workers find the fullerene shrinking process they observe in their simulations rather mysterious; yet it happens.

How Shrinking Arises. Can the concept of thermal shrinking of large fullerenes be used to create an explanation of the high yield synthesis of C_{60} and C_{70} in the presence of reasonably high pressures of buffer gas at temperatures of a few thousand Kelvin? The problem in such a system is that the equilibrium constant for loss of C_2 from a fullerene is very small even at several thousand degrees. Thus, the background of C_2 from C_2 loss processes would create the back reaction and stop the process. Because larger fullerenes are more stable than smaller ones, it would appear that smaller fullerenes would not shrink to create a high yield of C_{60}.

The assumption needed to make the shrink mechanism work is that at high temperatures (>2000 K) reactions between fullerenes have a very small cross-section because the energy

binding two fullerenes together is small so that the entropy gained by separating them is dominant. The larger fullerene that could be created from the colliding fullerenes by rearranging many bonds does represent a major energy lowering, but such a complex, high activation energy process is only very rarely feasible. Thus, reactions between fullerenes in Morokuma's second stage of annealing must be carried primarily by exchange of small carbon species with C_2 most likely the dominant species exchanged. (Whereas C_3 is more stable per carbon atom than C_2, its loss does not leave a fullerene. In previous work, one of us (GES) searched for a C_3 loss mechanism without success.)

$$C_i \rightarrow C_{i-2} + C_2 \tag{5}$$

$$C_j + C_2 \rightarrow C_{j+2} \tag{6}$$

giving as an overall process

$$C_i + C_j \rightarrow C_{i-2} + C_{j+2} \tag{7}$$

It is reaction (6) that keeps the concentration of C_2 low, thereby allowing the shrinking process (5) to continue. It provides the driving force for the evolution of the cluster distribution. The shrinking giant fullerene that was the subject of the movie[11] illustrates this. It was entrapped inside a multiwall carbon nanotube. The C_2 being emitted presumably was reacting with the tube wall and being incorporated into it.

The equilibrium constants for reactions like (7) must now be estimated. The general trend of these energies per carbon (Figure 1) approaches that of a graphene sheet according to eq 2, which we can rewrite for the overall energy of a fullerene of size n as

$$E = E_v + \sqrt{n}E_e + nE_f \tag{8}$$

Thus, for generic fullerenes the energy change in reaction (7) is

$$\Delta E_7 = E_e(\sqrt{j+2} - \sqrt{j} + \sqrt{i-2} - \sqrt{i}) \tag{9}$$

where the constant term in eq 8 is canceled because there are two species on each side of eq 7 and the term linear in n is canceled because the number of carbon atoms is the same on each side of eq 7. If both i and j are much larger than 2, the normal square root expansion $\sqrt{(a+\delta)} = \sqrt{a}(1 + \delta/(2a))$ can be introduced to give

$$\Delta E_7 \approx E_e\left(\frac{1}{\sqrt{j}} - \frac{1}{\sqrt{i}}\right) \tag{10}$$

For $j = 225$ and $i = 64$, $\Delta E_7 = -2.4$ kJ/mol, which is almost negligible at 4000 K. In summary, the term in E_e favors slightly reactions in which large clusters get larger while small clusters simultaneously shrink. In the calculations below, we use eq 1, where ΔE_7 is zero, ignoring eq 10 because this simplifies the calculations somewhat. The direction of difference is such that eq 10 actually favors the process we propose.

The overall equilibrium constant for reaction (eq 7) is given by

$$\frac{C_{i-1}C_{j+1}}{C_iC_j} = \left[\frac{m_{i-1}m_{j+1}}{m_im_j}\right]^{3/2}\left[\frac{q_{i-1,\mathrm{int}}q_{j+1,\mathrm{int}}}{q_{i,\mathrm{int}}q_{j,\mathrm{int}}}\right]\exp\left[-\left(\frac{\Delta E_7}{RT}\right)\right] \tag{11}$$

where ΔE_7 is the ground-state energy difference, which is slightly smaller than zero for fullerenes on the energy curve of Figure 1 as demonstrated in (10) and $q_{\mathrm{int}} = q_{\mathrm{el}}q_{\mathrm{rot}}q_{\mathrm{vib}}$ and these q's are individual molecule partition functions. The leading factor in right-hand side of (11) arises from q_{trans}. For $i,j \gg 1$, this factor is about 1 (for $i = j = 70$, it differs from one by less than a part per thousand). For large values of i and j, it easy to convince oneself that the ratio of the q_{int}'s is approximately unity as well except for the symmetry number that arises in q_{rot}. For the all ^{12}C isotopomer of $^{Ih}C_{60}$, the symmetry number is 60 and for the all ^{12}C isotopomer of D_{5h} C_{70} it is 10. High symmetry reduces q_{rot} by division by the symmetry number. However, the special stability of these molecules (i.e., low energy) causes equilibrium constants for reactions like eq 7, leading away from them to be much less than unity.

As fullerene cages increase in size, the number of isomers containing a given number of carbon atoms increases rapidly. For C_{60}, there are a total of 1812 fullerene isomers, and by C_{100} there over 570 000.[13] At C_{100}, there are close to 900 isolated pentagon isomers.[13] For reactions like eq 7, the important consideration is not these individual numbers but the ratio of adjacent numbers. For the C_{98}, C_{100} pair including fullerenes with adjacent pentagons, this ratio is about 461/570.[13] In addition, many isomers may have too high an energy to play a significant role.

By assuming an initial distribution of concentrations for which C_{60} and C_{70} are not especially high and that eq 7 comes to equilibrium, introducing two stoichometric constraints

$$\sum C_i = \sum C_i^0 \tag{12}$$

where the C_i^0 are concentrations of the initial distribution of fullerenes. (This equation arises from eq 7 not changing the *number* of fullerenes),

$$\sum iC_i = \sum iC_i^0 \tag{13}$$

(arising from the fact that reactions like eq 7 do not change the center of gravity of the concentration distribution), a well-defined quasi-equilibrium problem is created. Here, the modifier "quasi" is introduced to indicate that all reactions of eq 7 are in equilibrium but not reactions like eq 3 or reactions fusing two large fullerenes. High yields of $^{Ih}C_{60}$ and $D_{5\,h}$ C_{70} are obtained because the energies of both of these species are well below the general trend curve in Figure 1. This makes their disproportionation constants (reaction eq 7 with $i = j = 60$ or 70) of these species small.

Qualitatively one expects those species whose energies fall well below the trend line of Figure 1 to have a high concentration predicting that $^{Ih}C_{60}$ and $^{D5h}C_{70}$ should reach a high concentration. However, as long as the starting distribution mean is above these species, the sum of the $^{Ih}C_{60}$ and $^{D5h}C_{70}$ mole fractions can never exceed 0.5 because for each molecule of this type produced by eq 7, another species of size larger than the mean of the initial distribution must be created. The actual values of the $^{Ih}C_{60}$ and $^{D5h}C_{70}$ mole fractions will obviously be temperature dependent. Their sum will decrease as the temperature increases as the increased entropy associated with the population of many species starts to dominate the energetic effects that favor $^{Ih}C_{60}$ and $^{D5h}C_{70}$. It turns out that the ratio of the mole fraction of $^{D5h}C_{70}$ to $^{Ih}C_{60}$ at quasi-equilibrium will increase with increasing temperature for the same reason.

Modeling Calculations

The easiest way to solve this problem numerically is to recognize that the equilibria are dynamic and to solve the kinetic equations of approach to equilibrium. With this approach, the stoichiometric constraints are automatically satisfied. The equilibrium constants are the ratios of the forward and backward reaction ($K_7 = k_{\mathrm{forward}}/k_{\mathrm{backward}}$), knowing the equilibrium constants provide information only about this ratio and no

TABLE 1: Isomerization Equilibrium Constants of Most-Abundant Fullerenes[a]

T	K $^{Ih}C_{60}$	K $^{D5h}C_{70}$
1000	5×10^{13}	1×10^{9}
1500	3×10^{8}	5×10^{5}
2000	9×10^{5}	1×10^{4}
2500	3×10^{4}	1×10^{3}
3000	2×10^{3}	2×10^{2}
3500	4×10^{2}	7×10^{1}
4000	1×10^{2}	3×10^{1}

[a] The reactions are for the isomerization of $^{Ih}C_{60}$ and $^{D5h}C_{70}$ to an isomer of the same size on the trend curve of Figure 1.

information about the absolute values of the rate constants, but this does not matter if the kinetic calculation is integrated in time to equilibrium. Because annealing times may not be long enough to reach equilibrium, the kinetic approach also has the advantage of providing cluster distributions as a function of time if values of $k_{forward}$ or $k_{backward}$ are assumed. The time behavior of the system also reveals where kinetic bottlenecks are preventing the achievement of equilibrium.

Such kinetic calculations are easily carried out using Matlab and its ode15s integrator. These can be started from any initial distribution but it seems most instructive to start with just a single fullerene cluster populated, which was arbitrarily chosen to be C_{154}. This permits the observation of the cluster distribution spreading as the reactions proceed. Initially the calculations were carried out using $k_{forward} = k_{backward} = 1$ for the all of the disproportionation reactions.

$$2C_i \rightleftharpoons C_{i-2} + C_{i+2} \tag{14}$$

except for the special cases of $i = 60$ and 70. For $i = 60$ and 70, the equilibrium constant is calculated from

$$\frac{C_{i-1}C_{i+1}}{C_i^2} = K_i = \left(\frac{\sigma_i^2}{\sigma_{i-1}\sigma_{i+1}}\right) \exp\left[-\left(\frac{\Delta E_0}{RT}\right)\right] \tag{15}$$

where the ΔE_0 is the distance of $^{Ih}C_{60}$ or $^{D5h}C_{70}$ from the curve as calculated from the energies of C_{58}, C_{60}, and C_{62} or from the energies of C_{68}, C_{70}, and C_{72} of Figure 1. However, because $K_{70} \ll 1$, the formation of species smaller than C_{70} is effectively blocked on any reasonable time scale because the reactions of type (eq 7) cannot skip over a cluster. However, because there are many (16 091) different C_{70} clusters[13] the original C_{70} species created is unlikely to be D_{5h} C_{70}. Thus, a more appropriate model is to use $K_{70} = 1$ (and $K_{60} = 1$) for the disproportionation reactions and introduce separate isomerization reactions

$$C_{70}\text{ (initial isomer)} \rightleftharpoons {}^{D5h}C_{70} \tag{16a}$$

$$C_{60}\text{ (initial isomer)} \rightleftharpoons {}^{Ih}C_{60} \tag{16b}$$

with equilibrium constants given by

$$K_{13} = \left(\frac{1}{\sigma}\right) \exp\left[-\left(\frac{\Delta E_0}{RT}\right)\right] \tag{17}$$

σ is the symmetry number of $^{D5h}C_{70}$ (or $^{Ih}C_{60}$) and the symmetry number of the generic C_{60} or C_{70} is assumed one. ΔE_0 is calculated from the distance of $^{D5h}C_{70}$ (or $^{Ih}C_{60}$) from the curve of Figure 1 multiplied by 70 (or 60). These equilibrium constants are given in Table 1 as a function of temperature. Later, it is shown that Table 1 predicts that the ratio of $^{Ih}C_{60}$ to $^{D5h}C_{70}$ increases at equilibrium as the temperature is lowered. The ratio of $^{Ih}C_{60}$ to $^{D5h}C_{70}$ is expected to be roughly the ratio of the left K to the right K in Table 1. This changes from a factor of 3 at 4000 K to 50 000 at 1000 K.

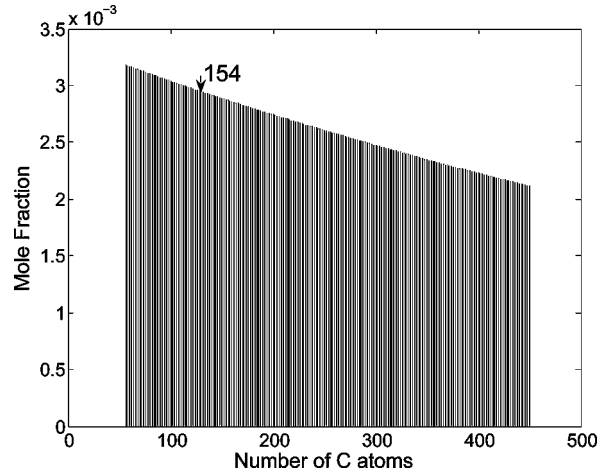

Figure 2. Equilibrium distribution of fullerene isomers after very long integration omitting $^{Ih}C_{60}$ and $^{D5h}C_{70}$. This distribution is shaped by the fact that only allowed sizes are between C_{56} and C_{450}.

An equilibrium calculation has been carried out. For this, the temperature was taken to be 4000 K and appropriate equilibrium constants for the reactions (eqs 16a and eq 16b) were introduced. The rates of the all reactions were assumed unity except for the backward reactions (eq 16a) and (eq 16b), which were calculated from the equilibrium constants and unit forward reactions. Initially, only C_{154} was populated with unit concentration. The allowed possible fullerene sizes ranged from C_{56} to C_{450}. To determine the equilibrium behavior, the integration was run out to 10^{10} time units. Even after this long integration, the two stoichiometric constraints are reasonably accurately satisfied, indicating that numerical stability is satisfactory. The final mole fraction of $^{Ih}C_{60}$ is 0.383 and of $^{D5h}C_{70}$ is 0.103. The sum of these mole fractions is 0.487 compared with maximum possible value of 0.5. The remaining mole fractions are distributed over the 198 other species. The mole fraction of $^{Ih}C_{60}$ divided by the mole fraction of $^{D5h}C_{70}$ is 3.71, to be compared with the 3.67 ratio of the equilibrium constants at 4000 K in Table 1 (calculated without the rounding of the table). Note that lowering the temperature would increase the ratio of $^{Ih}C_{60}$ to $^{D5h}C_{70}$ (Table 1). These ratios are expected to be approximately the same because the concentration of the generic C_{60} is nearly the same as that of the generic C_{70} as shown in the equilibrium distribution of all other species in Figure 2. *If the argument is accepted that the product of the first two factors in square brackets on the right-hand side of eq 11 is close to unity and the energies are taken from quantum chemical calculations (Supporting Information), there are no adjustable parameters in this equilibrium calculation.*

$^{Ih}C_{60}$ and $^{D5h}C_{70}$ are eliminated from Figure 2 (but not the calculations) in order for the ordinate scale to be expanded enough to see the rest of the distribution. The Figure 2 distribution is really determined by the fact that no clusters smaller than C_{56} or larger than C_{450} have been included in the model. This distribution cannot resemble any experimental result because the range of accessible clusters has been artificially limited. The distribution in Figure 2 is biased toward smaller clusters because the initial distribution is all at C_{154}, whereas the center of the allowed clusters is at C_{225} and thus the tilt toward smaller clusters is needed to satisfy the stoichiometric conditions even though almost half the clusters are tied up in the unshown $^{Ih}C_{60}$ and $^{D5h}C_{70}$. If we had used the more accurate

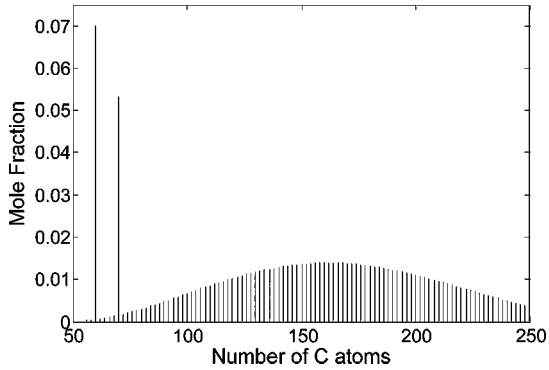

Figure 3. The distribution of the fullerenes for the case of Figure 2 at the time 1.06×10^7 units. This distribution resembles that of carbon arc fullerene soot. The distribution above C_{250} continues to taper off.

eq 2 instead of the less accurate eq 1, the main effect would have been a slight turning up of the distributions toward the extremes of Figure 2 because the ΔE_7 of eq 10 is more negative when i and j are separated by a large amount.

Distributions similar to those observed experimentally are observed at earlier times in the kinetic integration with this system. Figure 3 depicts the distribution after 1.06×10^7 time units. This resembles the fullerene distributions found in arc soots. The ratio $^{D5h}C_{70}/^{Ih}C_{60}$ is somewhat higher than is typical. However, in a kinetic calculation, this ratio is easily controlled by changing the forward and back reaction rate constants of eq 16a in tandem keeping the value of the equilibrium constant (eq 16b). To reduce the ratio $^{D5h}C_{70}/^{Ih}C_{60}$, either the temperature needs to be lowered or both rate constants of eq 16b need to be reduced. Lowering the rate constants reduces the fraction of the stream of carbon that is diverted into $^{D5h}C_{70}$ instead of flowing toward smaller clusters. We believe that almost any of the experimentally observed distributions can be reproduced through varying the temperature, the initial distribution, the individual rate constants (especially the constants affecting diversion into $^{D5h}C_{70}$), and the annealing time.

Discussion

Irle and Morokuma dubbed the mechanism revealed by their simulations "the shrinking hot giant." We believe a more appropriate name would be "spreading the distribution." Whatever it is called, this mechanism contrasts sharply with "the pentagon road" as an explanation of how high yields of buckminsterfullerene can be obtained. It seems unlikely that both will turn out to be valid. The experiments[3] Smalley carried out using a laser ablation of graphite inside a tube with heated walls provides control of a number of variables such as laser pulse energy, pulse duration, pulse wavelength, pressure, wall temperature, and graphite surface exposed. Whereas in principle there are many parameters available in this kinetic model, it is likely that the yields will be sensitive to only a tiny fraction of them. Perhaps the two models could be tested using cluster distributions from more controlled experiments such as these.

It is not clear whether this model can be applied to fullerene formation in combustion. If at some stage in the combustion process large fullerene-like structures are produced, then their distribution may be spread by annealing in the same manner as is described here. The concentrations of C_{60} and C_{70} found in the fullerene soots produced by combustion are quite similar to those found in pure carbon systems suggesting the mechanism proposed here might apply. However, it is believed that often soot produced earlier in the flame may be partially burned later. Thus, the fullerene concentrations in the soots produced in flames may be affected by the susceptibility of various species to oxidation, and the agreement between pure carbon and combustion distributions could be accidental.

Acknowledgment. This work was partially supported by NSF CHE-0807194 and the Welch Foundation. We would like to thank one of the reviewers of this article whose suggestion that we include the graphene sheet energy led to a valuable enrichment of the work.

Supporting Information Available: Ab initio energy calculations. This material is available free of charge via the Internet at http://pubs.acs.org.

References and Notes

(1) Vonhelden, G.; Gotts, N. G.; Bowers, M. T. *Nature* **1993**, *363*, 60.
(2) Gotts, N. G.; Vonhelden, G.; Bowers, M. T. *Int. J. Mass Spectrom.* **1995**, *149*, 217.
(3) Smalley, R. E. *Acc. Chem. Res.* **1992**, *25*, 98.
(4) Haufler, R. E.; Chai, Y.; Chibante, L. P. F.; Conceicao, J.; Jin, C.; Wang, L. S.; Maruyama, S.; Smalley, R. E. *Mater. Res. Soc. Symp. Proc.* **1991**, *206*, 627.
(5) Zheng, G.; Irle, S.; Morokuma, K. *J. Chem. Phys.* **2005**, *122*, 014708.
(6) Irle, S.; Zheng, G.; Wang, Z.; Morokuma, K. *J. Phys. Chem. B* **2006**, *110*, 14531.
(7) Irle, S.; Zheng, G.; Wang, Z.; Morokuma, K. *NANO FIELD* **2007**, *2*, 21.
(8) Zheng, G. S.; Wang, Z.; Irle, S.; Morokuma, K. *J. Nanosci. Nanotech.* **2007**, *7*, 1662.
(9) O'Brien, S. C.; Heath, J. R.; Curl, R. F.; Smalley, R. E. *J. Chem. Phys.* **1988**, *88*, 220.
(10) Huang, J. Y.; Ding, F.; Jiao, K.; Yakobson, B. I. *Phys. Rev. Lett.* **2007**, *99*, 175503.
(11) Xie, Z.-X.; Liu, Z.-Y.; Wang, C.-R.; Huang, R.-B.; Lin, F.-C.; Zheng, L.-S. *J. Chem. Soc., Faraday Trans.* **1995**, *91*, 987.
(12) Murry, R. L.; Strout, D. L.; Scuseria, G. E. *Int. J. Mass Spectrom. Ion Processes* **1994**, *138*, 113.
(13) Fowler, P. W.; Manolopoulos, D. E. *An Atlas of the Fullerenes*; Clarendon Press: Oxford, 1995.

JP806951V